Heliyon 6 (2020) e05549

Contents lists available at ScienceDirect

Heliyon

journal homepage: www.cell.com/heliyon

Research article

Numerical approach to minimize mercury contamination by geometric and parametric optimization

Pragati Shukla *, S. Manivannan, D. Mandal

Alkali Materials & Metal Division, Bhabha Atomic Research Centre, Trombay, Mumbai, 400085, India

ARTICLE INFO

Keywords:
Air pollution
Numerical methods
Mercury
Species transport
Ventilation
Engineering
Chemistry
Environmental science

ABSTRACT

Due to high vapour pressure at ambient conditions, exposed mercury contributes significant vapour concentration in working atmosphere. Ventilation is a conventional, cheap and very effective method to bring down the concentration of hazardous materials like mercury vapour below permissible limit. In this work a numerical model was developed to obtain intuitive understandings of the spatial distribution of mercury vapors from an exposed surface. The model was validated with experimental data generated using a precinct ventilation system with 8.14% absolute average error. a Validated model was used to study the effect of air flow rate (100–1200 LPM) and impact of architectural design of the containment for fixed exposed mercury surfaceon the final (diluted) mercury concentration. Comparative analysis shows that modification in structural design offers a reduced volume averaged exit mercury concentration and also the reduced peak mercury concentration(C_{peak}) in the computational domain. Computational approach outlined in this work can be used to estimate spatial variation of mercury vapor concentration and to locate and quantify regions of high local concentration of mercury in various geometries.

1. Introduction

Mercury is present in atmosphere, hydrosphere and biosphere. Because of good electrical and physical properties, it has innumerable industrial usages [1,2]. It is one of the major air pollutants and thus is a matter of concern for the environment, human and animal health [3,4,5,6]. Exposure to mercury may lead to acute and chronic intoxication resulting to various diseases like heart attack, central nervous system damage, kidney injuries to name a few [7,8]. Widespread usage of mercury demands for robust and reliable exposure measurement techniques as well as safe handling techniques. Mercury vapour concentration in air can be measured directly or indirectly. There are studies reporting atmospheric measurements in rural locations, terrestrial sites and over the oceans [9,10]. In atmosphere mercury exists in three forms viz. oxidized mercury, particle-bound mercury and elemental mercury [11]. Researchers have developed different methods for estimating different forms of mercury contaminations in air. For elemental mercury, atmospheric oxidation followed by adsorption, or deposition of reactive gaseous mercury, and particulate-phase mercury may lead to effective removal of mercury [12,13,14]. Poly sulfonecation-exchange membranes and foliar surfaces have also been used for mercury measurement [15]. Available sampling and analysis methods for three different forms of mercury have been compared in a study [16].

Once detected there must be robust strategies to ensure that mercury concentration in air stays below prescribed Threshold Limit Value (TLV). Several preventive actions can be taken in order to attain this objective and providing sufficient number of air changes is one of them. A good ventilation system can help in achieving acceptable worker exposure by diluting the contaminant concentration. Thus by having sufficient number of air changes (i.e. air flow rate) the mercury concentration can be brought below TLV (25μ gm/m3) [17]. The contamination depends on generation rate of contaminant i.e. mercury in present case and the air flow velocity [18]. Required air changes to reduce mercury contamination below permissible limits can be experimentally evaluated. Air flow rate and the rate of generation of mercury are the two most important parameters which determine concentration of mercury in air. The rate of formation of mercury depends on it's vapour pressure and the exposed surface area. Thus higher the surface area more will be the concentration. For designing an efficient ventilation system, understanding the interplay between these parameters is very important. There are very limited references are available for better local ventilation designs [19].

However the estimation of necessary air requirements for sufficient dilution till date is based on experimentation which is typically labor

* Corresponding author.
E-mail address: pragati@barc.gov.in (P. Shukla).

https://doi.org/10.1016/j.heliyon.2020.e05549
Received 11 May 2020; Received in revised form 4 September 2020; Accepted 16 November 2020

intensive and expensive as well. Moreover one cannot exclude chances of inadvertent exposure of personnel to relatively high dosage of mercury. In this context use of commercial CFD codes to arrive at expression for minimum air requirement for a given geometry of the work space becomes important. A CFD based model is also being used for designing inlet air ducts in a work space/floor. A validated CFD model can be used to simulate essential to provide a complete spatial profile of mercury concentration which can provide information on location of dead zones with high local concentrations. This information is crucial for the effect of a wide range of conditions as well as transients on the net resultant mercury contamination in a given workspace, constrained or otherwise. This not only reduces time and cost associated with experiments (that too a large number to rigourously ascertain a given geometry of workspace) but also reduces risk of contamination and accidental exposure to operating personnel. CFD simulations are highly reliable and commonly used in designs for industrial construction and building structures, environmental forecasting for urban planning, and the diffusion of pollutants [20]. However to the best of our knowledge there are no many reports on use of CFD to meet these requirements with respect to mercury vapors.

Recently researchers have tried to numerically model emission, transport, transformation and deposition of atmospheric mercury [21]. Mercury pollution is a growing concern from an environmental and epidemiological point of view. Community Multi-Scale Air Quality model (CMAQ) has been used by many researchers for simulating mercury emission, transport diffusion and transformation [22]. Readily available mathematical models for mercury transport mostly focuses on large distances (<50 km) which is not applicable for local impacts. There are only a few reports that focuses on Eulerian grid-based model and Gaussian plume modelthat can be used to calculate the atmospheric deposition of Hg in the vicinity (i.e., within 50 km) [23]. Recently commercial CFD codes have been used to numerically estimate spatial variation of contaminants/pollutants in a ventilated closed space. Such codes can be used to get a reasonably accurate estimate of the number of air changes required (and hence design an effective ventilation system) for a given load of contaminant. A CFD based approach was used to design a ventilation system to cater to management of CO gas in a car park [24]. Another three-dimensional flow field simulation investigates the impact of the architectural design of termite nest walls on CO_2 exchange, heat transport and water drainage using (CFD) software. The construction behavior of nest seems to select structures that provide advantages in terms of effective CO_2 ventilation and thermal regulation [25]. Recently a CFD model to predict behavior of mercury in air-coal and oxy-coal combustion systems has been reported [26]. The authors compared their results from CFD with the measurements from a pilot-scale test facility and reported reasonable agreement between the two. A CFD based approach to study the effect of air dilution through ventilation to reduce methane and other contaminants so as to provide sufficient air quality was also reported [27]. CFD has also been used by many other researchers to numerically study the effect of size and position of the inlet and outlet openings on the characteristics of the flow inside buildings, which can strongly influence the ventilation performance and the indoor air quality [28,29,30,31]. A case study for enhancing urban ventilation performance through the development of precinct ventilation zones was reported that could be useful for increasing wind-related knowledge in the context of real world [32]. In other reported study numerical transient simulations were used to investigate the air flow patterns, distribution and velocity, and the particulate dispersion inside an existing typical hospitalization room equipped with an advanced Heating Ventilation Air Conditioning (HVAC), with Variable Air Volume (VAV) primary air system designed for immune-suppressed patients [33]. It can be seen that numerical simulation have been effective approaches to mimicking wind environment in precincts and fully present the overall precinct ventilation performance of neighborhoods [34]. Even though there has been a large volume of work pertaining to use of CFD in estimating performance of ventilation system, similar work pertaining to mercury contamination is rare. Development of such CFD codes that can be used to design ventilation system specific to mercury contamination is all the more important given the toxic nature of the element. This work aims to fulfill this gap area. Recently we reported effect of variation of air flow rate on exit concentration of mercury vapour in a cylindrical geometry [17]. A CFD model was developed to numerically determine the exit concentration from first principles. The quantity of the mercury contaminant was kept fixed.

In present work we validate the developed numerical (CFD) model against experimental results. Thereafter we use the model to obtain study dependence of exit mercury concentration on air flow rates as well as the extent of initial mercury contamination. In addition to this, effect of geometry of the enclosure was also studied. CFD simulations revealed that geometry of the enclosure has a important influence on the exit mercury concentration for a given air flow rate and given extent of initial mercury contamination. Also this study clearly shows how CFD can be an important tool to arrive at an optimum geometry (for a given extent of mercury contamination) if the air flow is a constraint or to arrive at the required air flow rate if the geometry is a constraint.

2. Experimental setup, computational approach and domain

2.1. Experimental setup and computational domain

Experiments were conducted using an acrylic cylinder of diameter 40 mm and height 475 mm. The base of the cylinder was covered with mercury. 15 NB nozzle was provided on one side of the cylinder at a height of 2 cm for the base. The inlet air line was 10 mm above mercury level in the column. The top portion of the cylinder was connected to an outlet line where in a mercury vapor analyzer was installed. A commercial mercury sampler with a gold film was used. The gold film in effect precipitates the atmospheric mercury and forms an amalgam. Instrument regeneration was simply by electrical heating which breaks the amalgam. Use of such gold sensor or gold quoted diffusion screen is quite common for mercury concentration measurements [35]. Moisture free air was pushed into the system using a compressor at a desired flow rate. Flow rate was maintained using a calibrated rotameter. Figure 1 shows the experimental setup. The set up was operated until steady state was attained. Some preliminary experiments showed that 3–4 number of air changes (corresponding to the cylinder volume) was sufficient to ensure that the exit concentration of mercury (at the location of the analyzer) was constant and did not deviate. All experimental readings were taken after waiting for a time corresponding to 10 air changes. The experiments were carried out to ascertain the outlet mercury concentration for different flow rates of air. The results of experiments were used to validate the computational model detailed below.

2.2. Computational approach

The concentration contour of mercury across the domain was obtained from first principles. A two-step computational approach was followed in this work. In the first step, Navier-Stokes equations as applicable for steady-state incompressible flow are solved so as to arrive at the steady state flow field in the computational domain for a particular air flow rate. For the range of air flow velocity studied in this work maximum value of Re was 54.3 which ensured laminar flow conditions. Figure 2 shows the computational domain.

The governing equations for this step are:

Continuity equation:

$$\nabla.v = 0 \tag{1}$$

Momentum equation:

$$\rho v.\nabla.v = \mu\nabla^2 v - \nabla p + \rho g \tag{2}$$

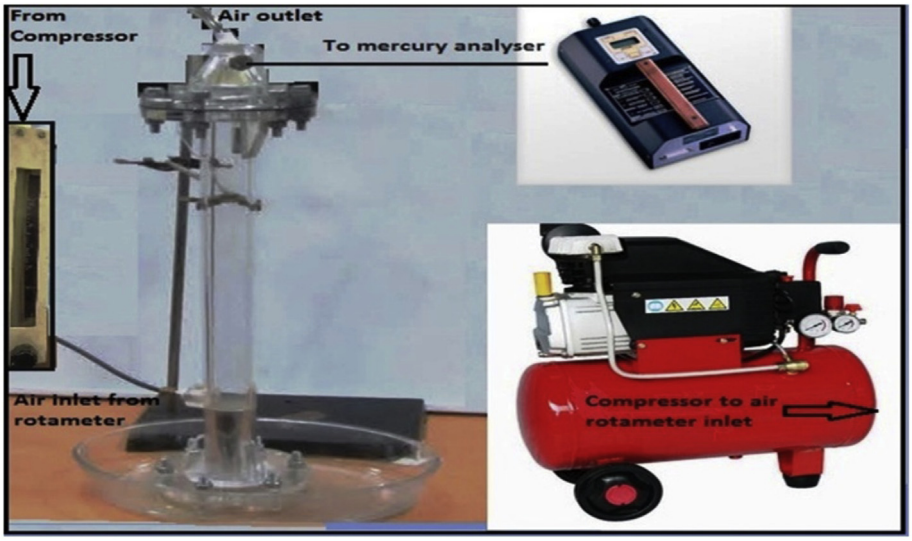

Figure 1. Experimental setup for obtaining effect of air flow rate on mercury concentration.

$$\frac{\partial \varnothing}{\partial t} + \overline{v}.\nabla \varnothing = D\nabla^2 \varnothing \quad (3)$$

Where p is the static pressure, term ρg is gravity induced body force and v is the velocity vector. Solution of Eqs. (1) and (2) in the first step of simulation gives local values of velocity components and pressure. The air inlet at the bottom of the cylindrical geometry (Figure 2) is defined as velocity inlet. The outlet is defined as pressure outlet (pressure kept at ambient conditions) while a no-slip boundary condition was defined at the cylindrical wall of the geometry. Having obtained the flow field a convection diffusion equation was solved so as to obtain the concentration profile of mercury. This equation is as follows. Where, ∅ is the value of the scalar (in this case mercury) which is transported across the computational domain by advective flow. D_{eff} is the effective diffusion coefficient. Under laminar flow conditions where in mass transport due to random movement of eddies are negligible and especially for a gaseous system D_{eff} can be considered to be primarily governed by values of molecular diffusivity.

Table 1 provides value of physical property of used in this work.

With regard to the species transport equation a zero concentration boundary condition was at the air inlet while a zero pressure gradient was used at the outlet. At the base of the geometry a constant flux boundary condition was defined. The method of estimating value of flux at ambient temperature is detailed in our previous work [17]. 'Detailed boundary conditions' provided as supplementary material may please be referred for more details of governing equations and boundary conditions.

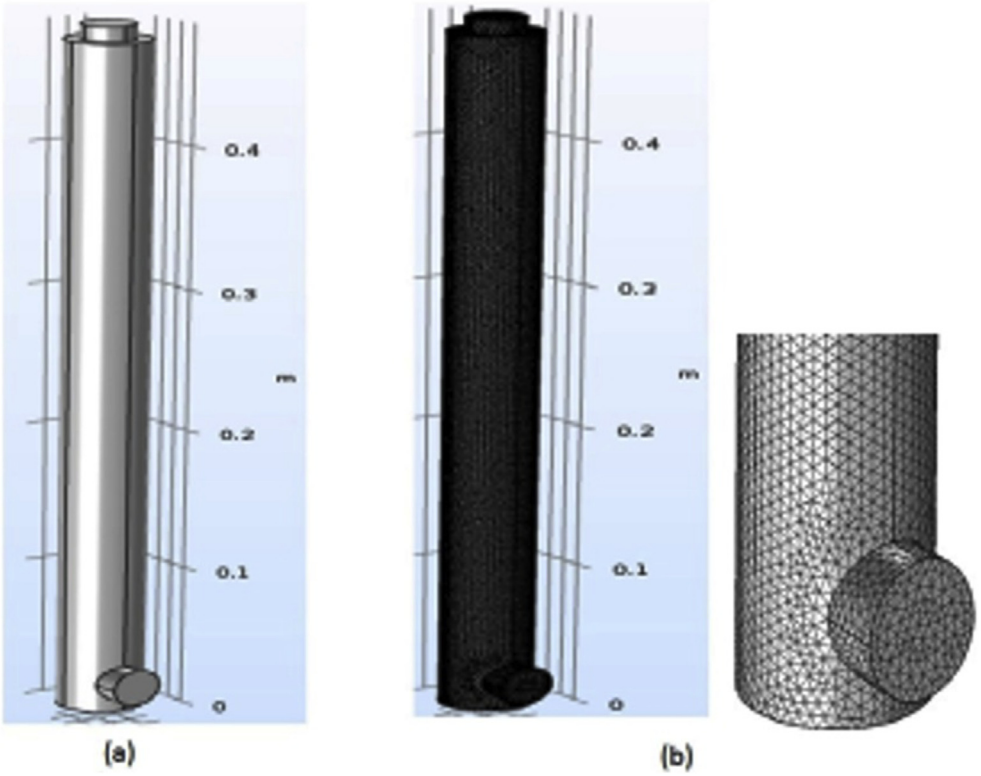

Figure 2. a) Computational domain and b) Meshed geometry used in the present work.

Table 1. Different parameters used in the simulation.

Molecular diffusion coefficient of mercury (m^2/sec)	Density of air (kg/m^3)	Viscosity of air (kg/m-sec)
12.6×10^{-6}	1.225	1.81×10^{-5}

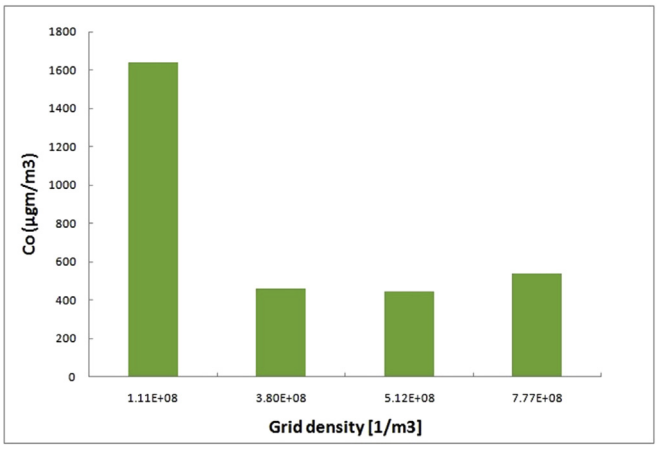

Figure 3. Grid independency test.

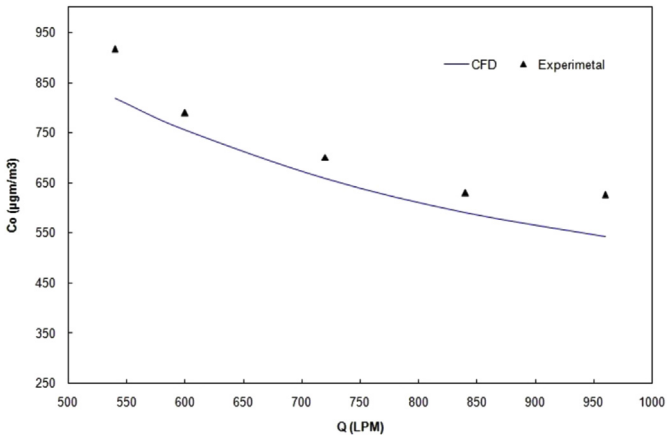

Figure 4. Validation of CFD model against experimental results.

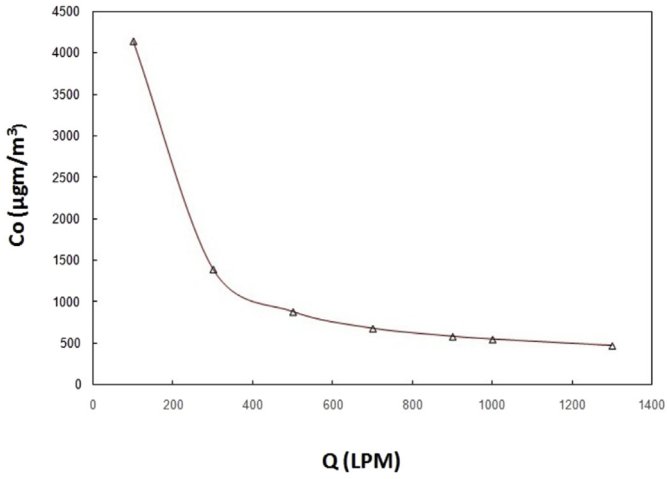

Figure 5. Effect of air flow rate (Q) on exit mercury concentration.

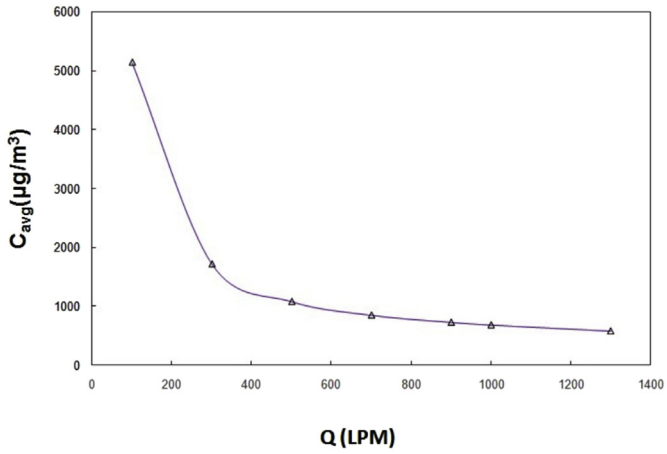

Figure 6. Effect of air flow rate (Q) on exit mercury concentration.

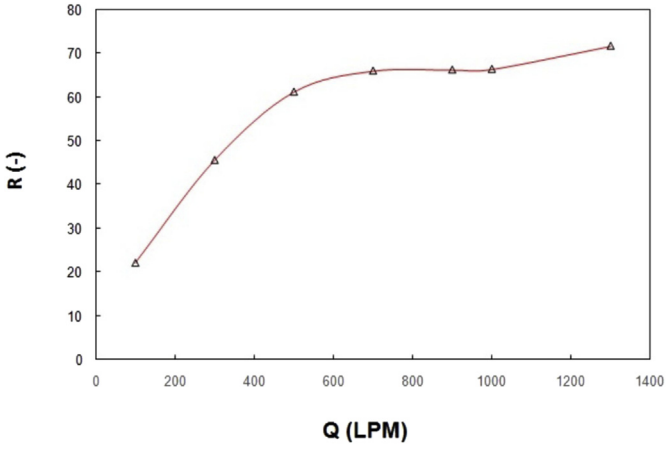

Figure 7. Effect of air flow rate on R.

As mentioned earlier four different geometries were tested in this work. The boundary conditions used for Navier-Strokes equation and species transport equation holds for all of the geometries.

3. Results and discussion

3.1. Grid independency test and validation

The 3D computational domain was meshed with a tetragonal (unstructured) mesh. Mercury vapor was considered as a gaseous species

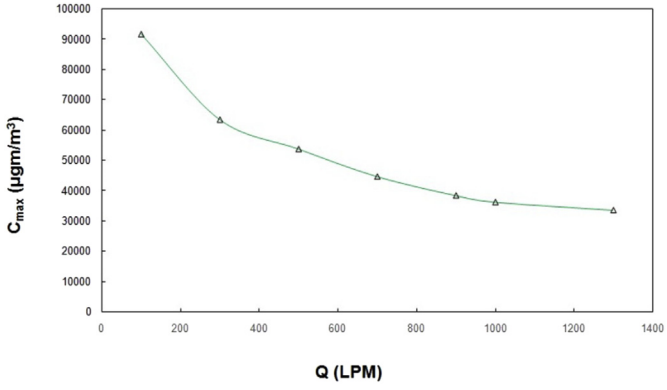

Figure 8. Effect of air flow rate on maximum concentration in computational domain.

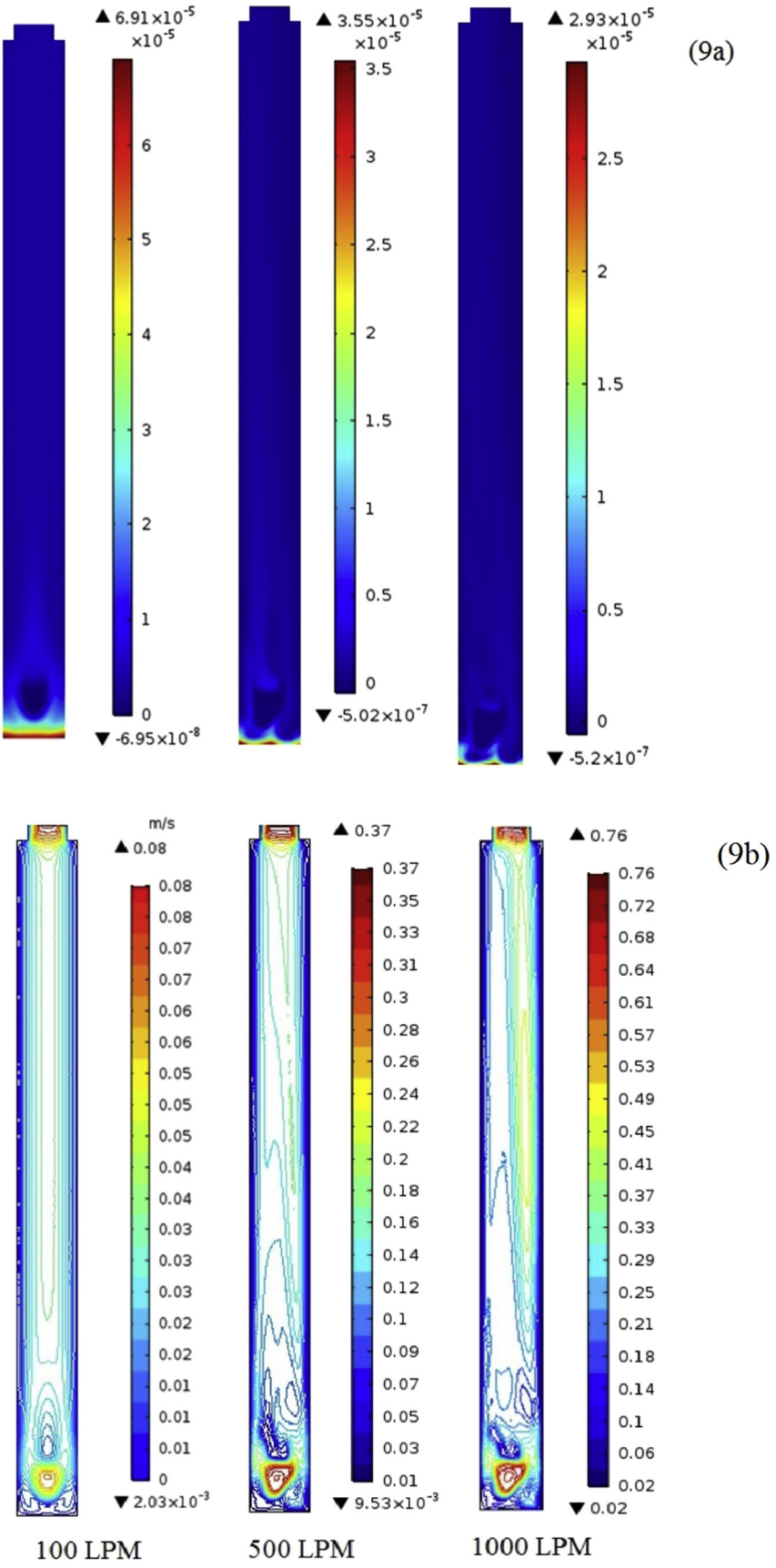

Figure 9. a) Mercury concentration contour and b) velocity streamlinesalong the height of the column for different values of air flow rate.

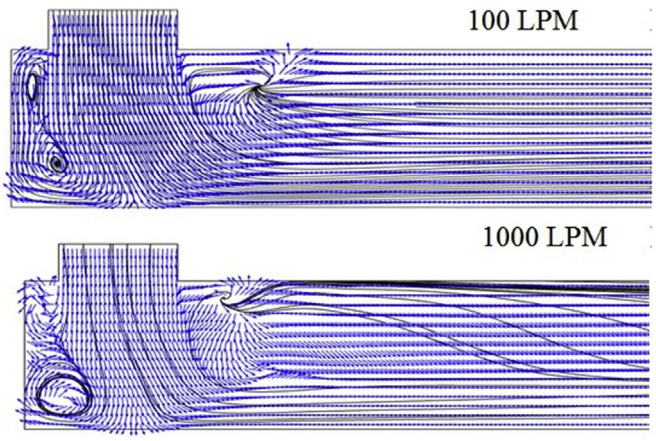

Figure 10. Velocity vector plot (and stream lines) at two flow rates.

being transported by convection and diffusion in the prevailing flow field of the incoming/injected air. At the onset a grid independency test was carried out so as to ensure that the grid size did not affect the results. Typically a sufficiently fine grid size is required so as to ensure the associated numerical diffusion does not surpass the molecular diffusion inherent to the system. As a gaseous system is being considered the magnitude of numerical diffusion should be lower even if a moderate grid density is being used. Four different grid densities were tested in this study - 1.11×10^8, 3.80×10^8, 5.12×10^8, and 7.77×10^8 cells/m^3. Figure 3 clearly shows that a grid density of 3.80×10^8 cells/m^3 is sufficient as there is no significant variation of the outlet concentration thereafter. Further simulations have been carried out using this grid density.

The developed CFD model was then validated against experimental data. Experiments had been carried out so as to obtain mercury concentration at the outlet for the set up for different air flow velocity rate in the range of 540–960 LPM. The numerical model was solved for exactly the same set of conditions (as in experiments) and the results of mercury concentration at the outlet of the computational domain were obtained. The results are compared in Figure 4.As can be seen from Figure 4, a good agreement between the predicted and experimental results is obtained. Absolute average error was 8.14 % while the maximum absolute error was 13.3 %. Hence the model developed in this work can be said to be accurate enough to capture the physics at play.

3.2. Effect of air flow velocity

One of the most important parameters that decide the outlet mercury concentration for a given extent of exposed mercury (ie for a given flux) is volumetric flow rate of air (Q). Higher the air flow rate more should be the reduction in outlet mercury concentration. For the cylindrical design as shown in Figure 2 simulations were carried out to test this. Figure 5 shows the results of these simulations. It can be seen that initially the rate of fall in mercury concentration is quite high which is followed by a region where in changes in Q does not have any significant effect on exit concentration. A higher air flow rate (for a given quantity of exposed mercury) translates to a higher extent of dilution leading to lower exit concentration.

Figure 6 shows the variation of volume averaged mercury concentration with air flow rate. This value represents average value of mercury concentration inside the cylindrical enclosure. It can be seen that as with increase in flow rate of air the volume averaged concentration of mercury also reduces due to increased dilution at higher air flows. However one important observation was that the value of average mercury concentration was consistently higher than that at the exit. This indicates presence of pockets of high local mercury concentration inside the cylindrical enclosure.

One extremely important parameter that has been studied in this work is the ratio of mercury concentration at the outlet to the maximum mercury concentration in the computational domain. This parameter is a measure of local spikes in mercury concentration within the domain which are typically associated with persistent flow pattern in the domain. This information on local over concentration of mercury is extremely important and is provided by CFD models. Hence in a given domain there can exist pockets where in local concentration of mercury can be many a times higher than average concentration and can exceed stipulated limits. CFD solves the flow field and provides a reasonably accurate contour of mercury vapor concentration across the entire domain of interest.

Figure 7 shows the ratio of mercury concentration at the outlet to the maximum mercury concentration in the computational domain (R) for different values of air flow rate. It could be seen that values of R can be as high as 71.7. An increase in flow rate was infact seen to increase R. The rate of rise of R was high at low value of Q while it became almost constant for value of Q greater than 700 LPH. Thus the local (peak) values of mercury concentration inside the domain could be significantly higher (by as much as two orders of magnitude) than the average concentration (at exit). Figure 8 shows the maximum mercury concentration across the computational domain for different flow velocities. Results show the peak values of mercury concentration is much higher than exit concentration as well as volume averaged concentration. This is primarily attributed to the formation of pockets of very high local mercury concentration.

At this point it is important to understand the reason behind a non uniform contour of mercury concentration (which essentially leads to a value of R significantly greater than unity) and how air flow rate affects that contour. Figure 9 (a) shows the mercury concentration contour along the height of the computational domain for three different values of air vol. flow rate (100 LPM, 500 LPM and 1000 LPM). Figure 9 (b) shows the velocity streamlines under these conditions.

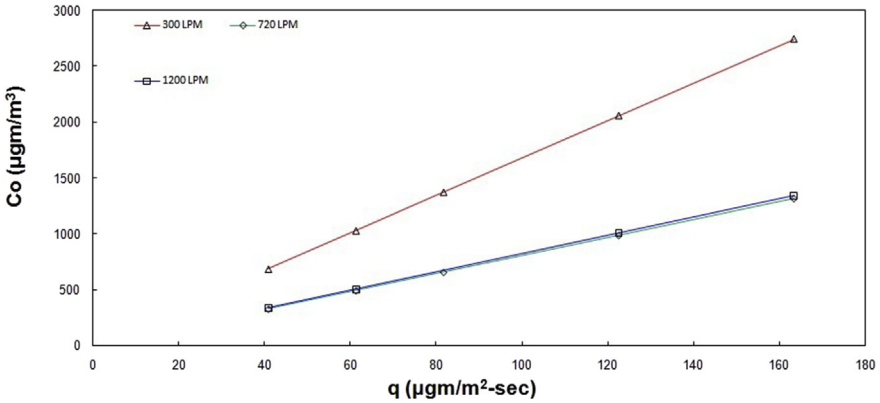

Figure 11. Effect of mercury flux on exit mercury concentration for different air flow rates.

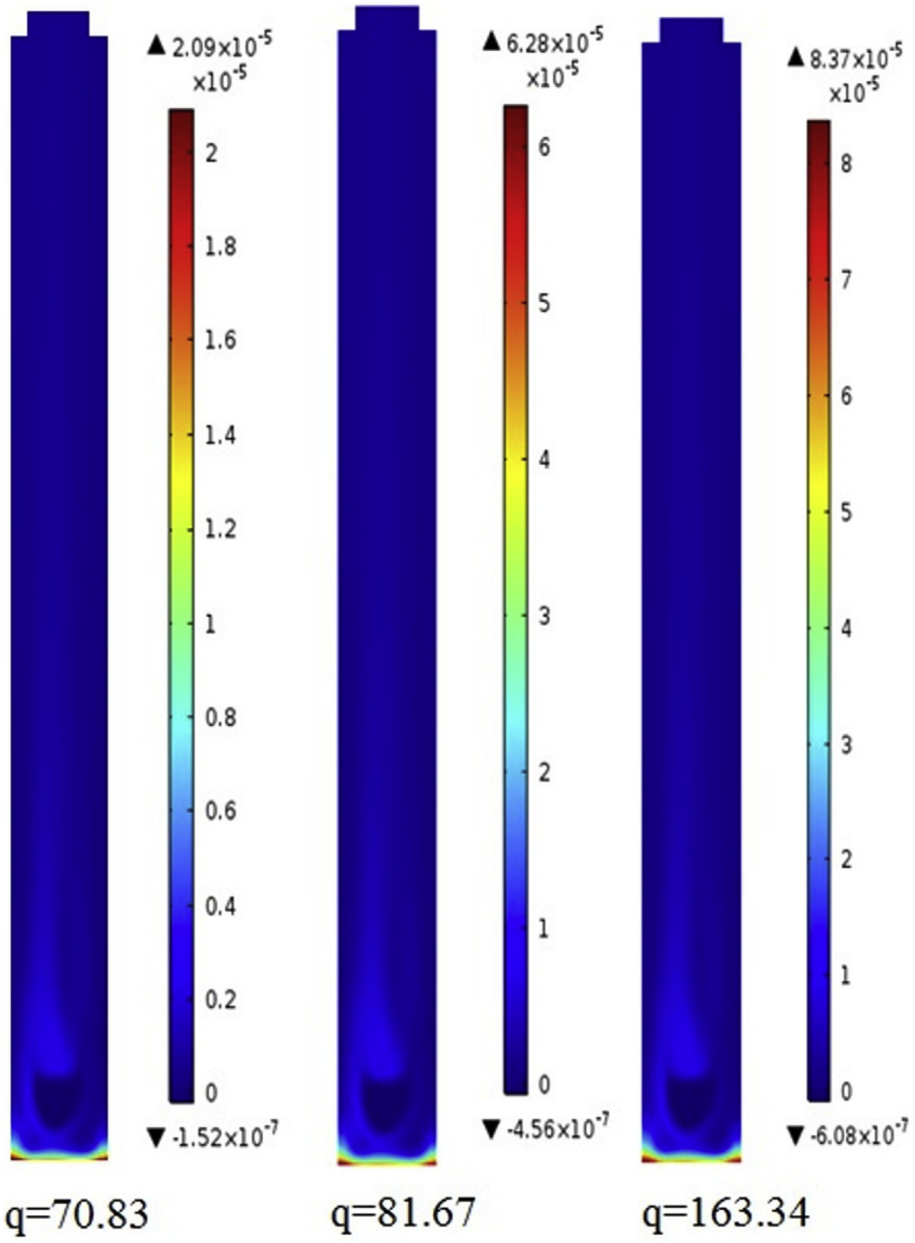

Figure 12. Concentration contour at three different values of mercury flux.

The plane considered is perpendicular to the air inlet port. It can be seen from Figure 9 that the maximum (peak) concentration of mercury occurs in the region just above the exposed surface and below the air inlet. The contour is symmetric at a flow rate of 100 LPM but becomes more and more asymmetric as the air flow rate is raised. Also it can be seen that the region of higher concentration is more wide spread at low values of air flow rate and tends to reduce as the air flow rate is raised. Figure 9 b shows the velocity streamline plot for the three cases. The zone of higher velocity streamline corresponds to the location of the air inlet port. One important observation is that at low flow rates the streamlines are symmetric which is explains the symmetric nature of the concentration contour plots in Figure 9a. As flow rate is increased the streamlines lose their symmetry which directly reflects on the concentration contour.

Analysis of the velocity vector plot in Figure 10 reveals that the zone of peak concentration is essentially a dead zone. The fluid in this zone does not communicate with the main flow. However the fluid is also not static as well and is moving in form of a re circulation which does not intersect the main flow streamlines. Thus the transport of mercury species form this zone to the main flow zone is mostly due to diffusive transport. There is not much of a convective transport which leads to relatively high value of concentration in this zone. As the flow rate is raised the span of this recirculation increases as is clearly seen. Thus as air flow rate is increased from 100 to 1000 LPM a wider dead zone forms. This in effect leads to formation of pockets of high local values of mercury concentration as the mercury species enclosed with in a dead zone becomes trapped and cannot communicate with the main flow (even though the main flow is much higher at 100 LPM). This explains the observation that with increase in flow rate (of air) the concentration of mercury is not reduced.

3.3. *Effect of flux*

For the cylindrical geometry considered in this work, further simulations were carried out to ascertain the effect of flux of mercury (q) on the exit mercury concentration. Figure 11 shows the effect. It could be

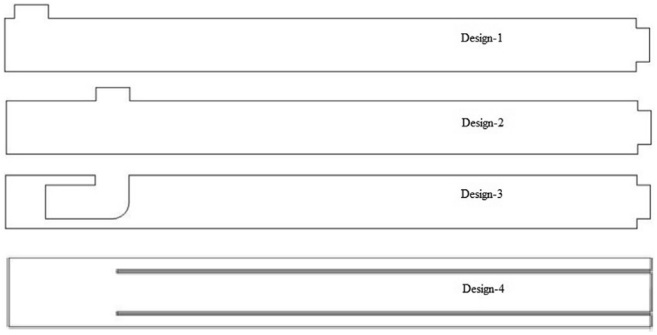

Figure 13. Geometries considered in the present work.

seen that exit mercury concentration increases monotonically with increase in mercury flux. Results were compared with three different values of flow rates. Once again exit concentration were significantly higher for a air flow rate of 300 LPM while there was no significant difference between 720 and 1200 LPM (higher ranges of flow rates). One important observation was that with increase in flux difference in exit mercury concentration for high and low values of air flow rate also increases.

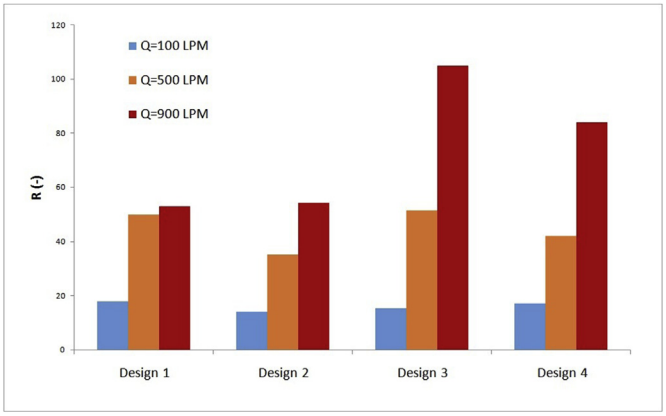

Figure 16. Effect of different designs of air inlet on peak mercury concentration in the computational domain.

Figure 12 shows the concentration contour plots for three values of mercury flux at a flow rate of 300 LPM. As the mercury flux is raised, the magnitude of the local concentrations keeps on increasing almost monotonically but the contour does not change significantly primarily

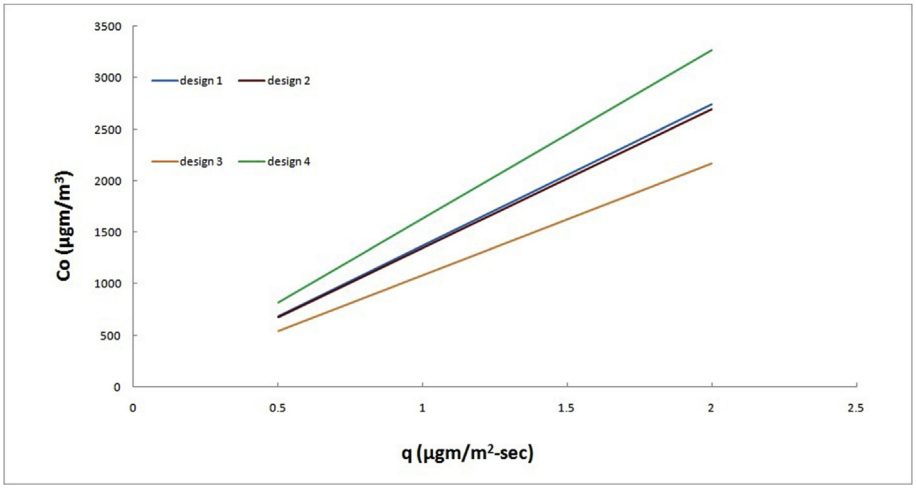

Figure 14. Effect of air flow rate on exit mercury concentration for different geometries.

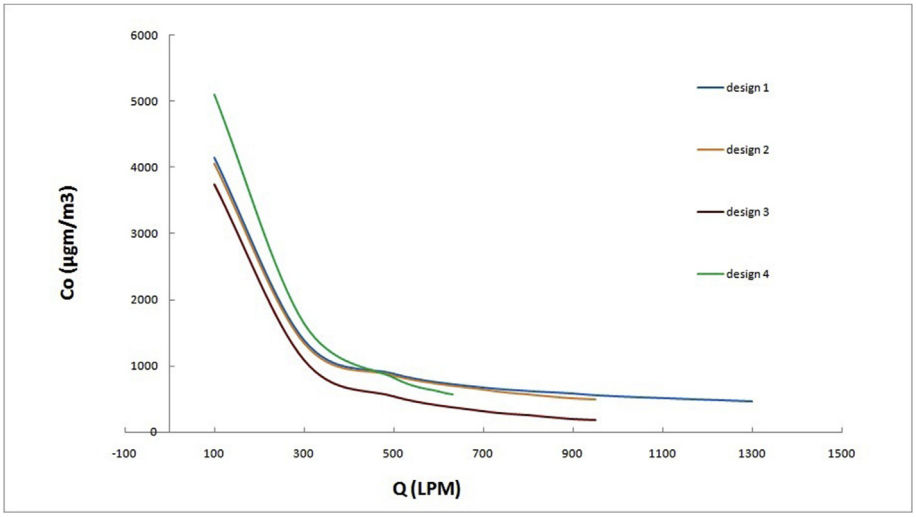

Figure 15. Effect of mercury flux on exit mercury concentration for different geometries.

because of the reason that the air flow rate was kept constant at 320 LPM. An increase in mercury flux in effect leads to a higher rate of mercury vapors being injected onto the computational domain thus leading to higher values of exit mercury concentration.

3.4. Effect of different orientation of air flow inlet

In previous section it was seen that both velocity and mercury flux has a profound effect on exit mercury concentration as well as on the ratio of maximum to exit mercury concentration. The original geometry considered in this work had the air inlet port on one side. In this section effect of different orientation of the air inlet port on exit mercury concentration and ratio of maximum to exit mercury concentration is studied. In addition to the original geometry three more geometries were studied. Figure 13 shows the outline of the different geometries compared in this section. In 2nd geometry a lateral air inlet port is used but the height of the port (from the bottom) is increased. In the 3rd design the air inlet port is from one side of the column but is oriented downwards. In the 4th design the air inlet is oriented vertically downwards. In design 3 and 4 the incoming air is directed right on to the exposed mercury surface and hence is expected to perform better as compared to the other designs.

Figure 14 shows the effect of air flow rate on the exit mercury concentration (volume averaged) while Figure 15 shows the effect of air flow rate on the mercury flux on exit mercury concentration for four different geometries considered in this work. It can be clearly seen from Figures 14 and 15 that the results (exit mercury concentration) for design 1 and 2 are quite similar both with variation of air flow rates as well as mercury flux. This is also expected as the orientation of the inlet air nozzles is similar in that the air flow is at right angles to the exposed mercury surface. However for the same air flow rate (Figure 14) and mercury flux (Figure 15) exit mercury concentration is the least for design 3. In design 3 the inlet air is directed right on to the exposed mercury surface and hence is more effective in removing mercury vapors from the exposed mercury surface. An increase in rate of mercury vapor removal in turn reduces the volume averaged exit concentration. The volume averaged exit mercury concentration for design 4 is however the highest (amongst all the designs) for low air flow rates but for relatively higher flow rates of air reduces to levels below that of design 1 and design 2.

Not only does design 3 offers a reduced volume averaged exit mercury concentration but also the peak mercury concentration in the computational domain (C_{peak}) is the least for this design. Figure 16 shows the comparison of C_{peak}values of the four different geometries studied in this work for three different air flow rates (ie. 100, 500 and 900 LPM). It can be clearly seen that valuesof C_{peak} is the highest for design 2 while it is the least for design 3. In design 2 the location of air inlet is higher than that in design 1 and thus the re-circulations created by sudden change of direction of the incoming air is not of sufficient strength so as to entrain and pick up mercury vapors close to the exposed mercury surface. This leads to higher values of C_{peak} in design 2. On the contrary in design 3 the injected air stream collides head on with the exposed mercury surface and is thus able to entrain the vapors close to the exposed surface leading to reduced peak concentration of mercury vapors.

Thus the computational approach outlined in this work can be used to estimate spatial variation of mercury vapor concentration which would enable one to locate and quantify regions of high local concentration of mercury in various geometries. Such model can very effectively be used to judge suitability of ventilation systems in enclosures where in there are chances for spillage of mercury.

4. Conclusions

A 3D numerical model was developed to study the effect of air changes on mercury contamination in an enclosure. The model was validated with experimental data. Absolute average error between predicted and simulated results was 8.14%. Not only the model could be used to predict exit mercury concentration for a given geometry of enclosure and for a given flow rate but the model could be used to obtain the spatial distribution of mercury vapor concentration so as to locate and quantify regions of local high mercury concentration. It was shown that the ratio of peak mercury concentration to that in the exit for a simple cylindrical geometry with lateral air inlet (geometry 1) can be as high as 71.7. In all cases exit mercury concentration was seen to reduce with increase in air flow rate due to dilution where the ratio of peak to exit concentration was seen to increase with air flow rate. The model was also used to predict the effect of mercury flux on the exit and local mercury concentrations. A linear dependence of exit mercury concentration with mercury flux was observed. Moreover the model was used to study the effect of variation of geometry of air injection. It was seen above that for all the designs exit mercury concentration reduced near exponentially with increase in flow rate. An increase in mercury flux however linearly increased exit mercury concentration. Both exit as well as peak mercury concentration was seen to be minimum for the design where in lateral air entry was bent downward so as to ensure the injected air stream hits the exposed head on (geometry 3). Thus the computational approach outlined in this work can be used to estimate spatial variation of mercury vapor concentration which would enable one to locate and quantify regions of high local concentration of mercury in various geometries. We believe that this work exemplifies the usefulness of numerical investigations to judge suitability of ventilation systems in real situations and provides important recommendations towards suitability of ventilation systems in enclosures where in there are chances of contamination of air via diffusion of an air pollutant.

Declarations

Author contribution statement

Pragati Shukla: Performed the experiments; Wrote the paper.

S. Manivannan: Conceived and designed the experiments; Wrote the paper.

D. Mandal: Contributed reagents, materials, analysis tools or data; Wrote the paper.

Funding statement

This work was supported by Bhabha Atomic Research Centre (BARC).

Data availability statement

Data included in article and supplementary material.

Declaration of interests statement

The authors declare no conflict of interest.

Additional information

Supplementary content related to this article has been published online at https://doi.org/10.1016/j.heliyon.2020.e05549.

Acknowledgements

Authors of this paper would also like to show her gratitude to Dr. Nirvik Sen, Chemical Engineering Division, BARC for his continuous help and software support.

References

[1] B.M. Reddy, N. Durgasri, T.V. Kumar, S.K. Bhargava, Abatement of gas phase mercury- recent developments, Cat, Rev. Sci. Eng. 54 (3) (2012) 344–398.

[2] N. Pirrone, G.J. Keeler, J.O. Nriagu, Regional differences in worldwide emissions of mercury to the atmosphere, Atmos. Environ. 30 (17) (1996) 2981–2987.

[3] R.J.C. Brown, A.S. Brown, R.E. Yardley, W.T. Corns, P.B. Stockwell, A practical uncertainty budget for ambient mercury vapor measurement, Atmos. Environ. 42 (10) (2008) 2504–2517.
[4] N. Pirrone, W. Aas, S. Cinnirella, R. Ebinghaus, I.M. Hedgecock, J. Pacyna, F. Sprovieri, E.M. Sunderland, Toward the next generation of air quality monitoring: mercury, Atmos, Environ. Times 80 (2013) 599–611.
[5] K. Kim, E. Kabir, S.A. Jahan, A review on the distribution of Hg in the environment and its human health impacts, J. Hazard Mater. 306 (2016) 376–385.
[6] M. Sergio, G.H. Silva, M.E.R. Islas, J.M. Reyes, G.S. Munguia, S.S. Valdez, R.G. Martinez, Total mercury in terrestrial systems (air-soil-plant-water) at the mining region of San Joaquin, Queretaro, Mexico, Geofisica International 52 (1) (2013) 43–58.
[7] E. Ha, N. Basu, S.B. Reilly, J.G. Dóre, E. McSorley, M. Sakamoto, H.M. Chan, Current progress on understanding the impact of mercury on human health, Environ. Res. 152 (2017) 419–433.
[8] J. Huang, M. Gustin, Use of passive sampling methods to understand sources of mercury deposition to high elevation sites in the western United States, Environ. Sci. Technol. 49 (2015) 432–441.
[9] F. Sprovieri1, N. Pirrone, R. Ebinghaus, H. Kock, A. Dommergue, A review of worldwide atmospheric mercury measurements, Atmos. Chem. Phys. 10 (2010) 8245–8265.
[10] X. Zhang, B. Shen, S. Zhu, H. Xu, L. Tian, UiO-66 and its Br-modified derivates for elemental mercury removal, J. Hazard Mater. 320 (2016) 556–563.
[11] J.Y. Lu, W.H. Schroeder, L.A. Barrie, A. Steffen, H.E. Welch, K. Martin, L. Lockhart, R.V. Hunt, G. Boila, A. Richter, Magnification of atmospheric mercury deposition topolar regions in springtime: the link to troposphericozone depletion chemistry, Geophys. Res. Lett. 28 (2001) 3219–3222.
[12] S.E. Lindberg, S. Brooks, C. Lin, K.J. Scott, T. Meyers, L. Chambers, M.S. Landis, R.K. Stevens, Formation of reactive gaseous mercury in the arctic:Evidence of oxidation of Hg° to gas-phase Hg-II compounds after arctic sunrise, Water Air Soil Pollut. 1 (2001) 295–302.
[13] S.E. Lindberg, S. Brooks, C. Lin, K.J. Scott, M.S. Landis, R.K. Stevens, M. Goodsite, A. Richter, Dynamic oxidation of gaseous mercury in the arctic troposphere at polar sunrise, Environ. Sci. Technol. 36 (6) (2002) 1245–1256.
[14] S.N. Lyman, M.S. Gustin, E.M. Prestbo, F.J. Marsik, Estimation of dry deposition of atmospheric mercury in Nevada by direct and indirect methods, Environ. Sci. Technol. 41 (6) (2007) 1970–1976.
[15] J. Munthe, I. Wangberg, N. Pirrone, A. Iverfeldt, R. Ferrara, R. Ebinghaus, X. Feng, K. Gardfeld, G. Keeler, E. Lanzillott, S.E. Lindberg, J. Lu, Y. Mamane, E. Prestbo, S. Schmolked, W.H. Schroeder, J. Sommar, F. Sprovieri, R.K. Stevens, W. Stratton, G. Tuncel, A. Urba, Intercomparison of methods for sampling and analysis of atmospheric mercury species, Atmos. Environ. 35 (2001) 3007–3017.
[16] P. Shukla, S. Manivannan, A. kumar, N. Sen, S.B. Roy, Determining Number of Air Changes for Cylindrical Geometry to Cater to Mercury Contamination, CHEMCON Conference, IIT G, India, 2015, p. 68.
[17] W.A. Burgess, M.J. Elellenbecker, R.D. Treitan, Ventilation for Control of the Work Environment, John Wiley & Sons, 2004.
[18] L. Merlier, F. Kuznik, G. Rusaouën, S. Salat, Derivation of generic typologies for microscale urban airflow studies, Sustain. Cities Soc. 36 (2018) 71–80.
[19] Peng Xie, Jun Yang, Huiying Wang, Yanfang Liu, Yaolin Liu, A New method of simulating urban ventilation corridors using circuit theory, Sustain. Cities Soc. 59 (2020) 102162.
[20] O. Russell Bullock Jr., Katherine A. Brehme, Atmospheric mercury simulation using the CMAQ model: formulation description and analysis of wet deposition results, Atmos. Environ. 36 (2002) 2135–2146.
[21] N. Pirrone, Mahaffey Kathryn R, Dynamics of Mercury Pollution on Regional and Global Scales, Springer, 2005.
[22] Christian Seigneur, Kristen Lohman, Krish Vijayaraghavan, John Jansen, Leonard Levin, Modeling atmospheric mercury deposition in the vicinity of power plants, J. Air Waste Manage 56 (6) (2006) 743–751.
[23] R. Al-Waked, N. Groenhout, L. Partridge, M. Nasif, Indoor air environment of a shopping Centre carpark: CFD ventilation study, Univers. J. Mech. Engin. 5 (4) (2017) 113–123.
[24] Kamaljit Singh, Bagus P. Muljadi, Ali Q. Raeini, Christian Jost, Veerle Vandeginste, Martin J. Blunt, Guy Theraulaz, Pierre Degond, The architectural design of smart ventilation and drainage systems in termite nests, Sci. Adv. (2019) EAAT8520.
[25] M. Gharebaghi, K.J. Hughes, L. Ma, R.T.J. Porter, M. Pourkashanian, A. Williams, CFD Modelling of Mercury Behaviour in Air-Coal and Oxy-Coal Combustion Systems CFD Centre, 2nd Oxyfuel Combustion Conference, 2014.
[26] S.A. Saki, J.F. Brune, G.E. Bogin Jr., J.W. Grubb, M.Z. Emad, R.C. Gilmore, CFD study of the effect of face ventilation on CH4 in returns and explosive gas zones in progressively sealed longwall gobs, J. S. African Inst. Mining Met. 117 (2017) 257–262.
[27] P. Karava, T. Stathopoulos, A.K. Athienitis, Airflow assessment in cross- ventilated buildings with operable facade elements, Build. Environ. 46 (2011) 266–279.
[28] R. Ramponi, B. Blocken, CFD simulation of cross-ventilation flow for different isolated building configurations: validation with wind tunnel measurements and analysis of physical and numerical diffusion effects, J. Wind Eng. Ind. Aerod. 104 (2012) 408–418.
[29] Y. Tominaga, B. Blocken, Wind tunnel analysis of flow and dispersion in cross-ventilated isolated buildings: impact of opening positions, J. Wind Eng. Ind. Aerod. 155 (2016) 74–88.
[30] Michael Francis, CFD Analysis of Airflow Patterns and Heat Transfer in Small, Medium, and Large Structures, Virginia Polytechnic Institute and State University, Thesis, 2014, pp. 1–113.
[31] Enhancing urban ventilation performance through the development of precinct ventilation zones: a case study based on the Greater Sydney, Australia Bao-Jie He, Lan Ding , Deo Prasad, Sustain. Cities Soc. 47 (2019) 101472.
[32] Carla Balocco, Pietro Lio, Assessing ventilation system performance in isolation rooms, Energy Build. 43 (1) (2011) 246–252.
[33] N. Antoniou, H. Montazeri, H. Wigo, M.K.-A. Neophytou, B. Blocken, M. Sandberg, CFD and wind-tunnel analysis of outdoor ventilation in a real compact heterogeneous urban area: evaluation using “air delay”, Build. Environ. 126 (2017) 355–372.
[34] K. Larjava, T. Laitinen, T. Kiviranta, V. Siemens &D. Klockow, Application of the diffusion screen technique to the determination of gaseous mercury and mercury (II) chloride in flue gases, Int. J. Environ. Anal. Chem. 52 (2006) 65–73.
[35] Pragati Shukla, Parametric optimization for adsorption of mercury (II) using self assembled bio-hybrid, J. Environ. Chem. Eng. 8 (2020) 103725. In this issue.